

DRL-Based Beam Positioning for LEO Satellite Constellations with Weighted Least Squares

Po-Heng Chou¹, Chiapin Wang², Kuan-Hao Chen², and Wei-Chen Hsiao²

¹Research Center for Information Technology Innovation (CITI), Academia Sinica (AS), Taipei 11529, Taiwan

²Department of Electrical Engineering, National Taiwan Normal University (NTNU), Taipei 10610 Taiwan

E-mails: d00942015@ntu.edu.tw, chiapin@ntnu.edu.tw, 61375063h@ntnu.edu.tw, 61275046h@ntnu.edu.tw

Abstract—In this paper, we propose a reinforcement learning based beam weighting framework that couples a policy network with an augmented weighted least squares (WLS) estimator for accurate and low-complexity positioning in multi-beam LEO constellations. Unlike conventional geometry or CSI-dependent approaches, the policy learns directly from uplink pilot responses and geometry features, enabling robust localization without explicit CSI estimation. An augmented WLS jointly estimates position and receiver clock bias, improving numerical stability under dynamic beam geometry. Across representative scenarios, the proposed method reduces the mean positioning error by 99.3% compared with the geometry-based baseline, achieving 0.395 m RMSE with near real-time inference.

Index Terms—LEO satellites, reinforcement learning, beam weighting, WLS positioning, NTN.

I. INTRODUCTION

The integration of terrestrial, aerial, and satellite segments into a unified ground-air-space architecture has emerged as a key enabler for future sixth-generation (6G) networks, promising seamless connectivity, low latency, and global coverage [1]. Among these, low Earth orbit (LEO) satellite constellations are particularly attractive due to their wide coverage, rapid revisit capability, and suitability for delay-sensitive services. However, their highly dynamic topology, interference-prone links, and constrained on-board processing capabilities present significant challenges for robust and energy-efficient service delivery [1]–[3].

Recent research has addressed these challenges from multiple perspectives. A Lyapunov-based beam management strategy was developed for LEO networks with random traffic arrivals and time-varying topologies, effectively reducing beam revisit times and handover frequency [2]. A multi-satellite beam-hopping framework was introduced to balance load and avoid interference in non-geostationary orbit (NGSO) constellations, significantly improving spectral efficiency [4]. Deep reinforcement learning (DRL)-driven handover protocols have been designed to eliminate measurement-report overhead, thereby reducing access delay and collision rates in regenerative-type LEO networks [5]. Cooperative beam scheduling and beamforming approaches in multi-beam LEO systems have shown positioning accuracy gains of up to 17.1% under Cramér-Rao lower bound (CRLB) criteria [6]. Reinforcement learning-based robust beamforming methods

for multibeam downlinks have also demonstrated resilience to imperfect channel knowledge [7]. In addition, cooperative beam-hopping control strategies in ultra-dense LEO constellations have been proposed to enhance time-difference-of-arrival (TDOA) positioning performance [8].

Beyond the physical layer, system-level frameworks have also been explored. A symbiotic radio approach using collaborative DRL has been proposed for intelligent resource optimization in non-terrestrial networks (NTNs) [3]. Standardization and system-level research on integrated terrestrial and non-terrestrial networks (TN-NTN) localization have highlighted key challenges in synchronization, interference, and robustness [1]. Moreover, federated learning (FL) frameworks have been investigated for NTNs to enhance scalability and privacy in multi-tier deployments [9].

Despite these advances, most existing solutions still rely heavily on explicit CSI or involve computationally intensive optimization, limiting real-time applicability for resource-constrained LEO platforms. Traditional statistical estimation methods, such as weighted least squares (WLS) [10], widely used in positioning problems, provide reliable accuracy but lack adaptability in dynamic multi-beam environments. Meanwhile, DRL has proven effective in sequential decision-making tasks [11], yet its integration with lightweight positioning remains underexplored in NTNs.

Motivated by these gaps, this work extends the use of DRL beyond prior studies that focused primarily on handover optimization [5], load-balanced beam hopping [4], or cooperative scheduling [6]. We adopt the DQN framework [11], which approximates the action-value function with deep neural networks to enable efficient decision-making in large state-action spaces. Unlike previous DRL approaches requiring explicit CSI or heavy network coordination, the proposed framework applies DQN for beam positioning in multiple-input multiple-output (MIMO) LEO systems and integrates it with a WLS estimator [10]. This design allows adaptive beam selection and weighting directly from uplink pilot responses, eliminating CSI estimation, achieving robustness under interference-prone and GNSS-denied conditions, and significantly reducing computational complexity compared to conventional optimization or deep learning baselines. While CRLB-based optimization offers theoretical bounds, it is analytically intractable for fast-varying beam geometry. Hence, an augmented WLS estimator is adopted, whose efficiency asymptotically approaches the

CRLB under Gaussian noise.

The main contributions of this paper are summarized as follows:

- A novel DRL-based beam positioning framework is proposed for MIMO LEO systems, extending the use of reinforcement learning beyond handover, beam-hopping, and cooperative scheduling to precise user positioning.
- The proposed DQN dynamically selects and weights satellite beams, while a WLS estimator computes user positions, enabling robust localization without explicit CSI estimation.
- The proposed framework substantially reduces computational complexity, enabling real-time deployment for resource-constrained LEO satellite platforms.
- Simulation results show that the proposed method achieves more than 99.3% reduction in positioning error compared to baseline approaches, particularly under interference-prone and GNSS-denied scenarios.

II. SYSTEM MODEL

A. Coordinate System and Beam Geometry

We consider a LEO satellite constellation that continuously illuminates the Earth through multiple narrow beams. Within a short observation window, the ground-projected centers of visible beams are denoted by $\{\mathbf{c}_i\}_{i=1}^M$ in a local East-North-Up (ENU) or Earth-Centered Earth-Fixed (ECEF) coordinate system. The unknown user terminal (UT) position is represented by $\mathbf{x} \in \mathbb{R}^{d \times 1}$, where $d = 2$ for planar and $d = 3$ for full-space positioning.

For the i -th beam, the line-of-sight (LoS) unit vector from the beam center to the UT is defined as [12]

$$\mathbf{h}_i \triangleq \frac{\mathbf{x} - \mathbf{c}_i}{\|\mathbf{x} - \mathbf{c}_i\|}, \quad i = 1, \dots, M, \quad (1)$$

where $\mathbf{h}_i \in \mathbb{R}^{d \times 1}$ and $d = 2$ or 3 depending on the positioning dimension. The beam geometry $\{\mathbf{c}_i, \mathbf{h}_i\}$ is assumed quasi-static within a 1–5 s window, updated by ephemeris and the scheduler.

B. Channel Model

Following the model in [6], the narrowband line-of-sight (LoS) channel between the satellite and the UT is dominated by a single deterministic path. Let $\mathbf{s}_i \in \mathbb{R}^3$ denote the satellite antenna phase-center position and $d_i = \|\mathbf{x} - \mathbf{s}_i\|$ the slant range between the satellite and the UT. Consider a uniform planar array (UPA) with $N_x \times N_y$ elements and total antenna count $N = N_x N_y$. The complex baseband channel vector of beam i is expressed as

$$\mathbf{g}_i = \beta_i e^{j\phi_i} \mathbf{a}_t(\varphi_i) \in \mathbb{C}^{N \times 1}, \quad (2)$$

where ϕ_i denotes the random phase uniformly distributed in $[0, 2\pi)$, $\mathbf{a}_t(\varphi_i)$ is the uniform planar array (UPA) [13] transmit steering vector at the departure angle φ_i , and β_i represents the large-scale channel gain defined as

$$\beta_i = \sqrt{\frac{G_t G_r}{L_i}}, \quad L_i = \left(\frac{4\pi f_c d_i}{c} \right)^2, \quad (3)$$

with f_c denoting the carrier frequency, c the speed of light, and G_t, G_r the transmit and receive antenna gains, respectively. The UPA steering vector is written as

$$\mathbf{a}_t(\varphi_i) = \mathbf{a}_x(\theta_i^x) \otimes \mathbf{a}_y(\theta_i^y), \quad (4)$$

where

$$\mathbf{a}_x(\theta_i^x) = \frac{1}{\sqrt{N_x}} \left[1, e^{-j\pi\theta_i^x}, \dots, e^{-j\pi(N_x-1)\theta_i^x} \right]^\top, \quad (5)$$

$$\mathbf{a}_y(\theta_i^y) = \frac{1}{\sqrt{N_y}} \left[1, e^{-j\pi\theta_i^y}, \dots, e^{-j\pi(N_y-1)\theta_i^y} \right]^\top, \quad (6)$$

and the direction cosines (θ_i^x, θ_i^y) are determined by the azimuth and elevation of the UT relative to the satellite.

Given a transmit beamforming vector $\mathbf{f}_i \in \mathbb{C}^{N \times 1}$ for pilot transmission, the received scalar pilot signal and its corresponding SINR are given by

$$y_i = \mathbf{g}_i^H \mathbf{f}_i x_i + \sum_{k \neq i} \mathbf{g}_i^H \mathbf{f}_k x_k + v_i, \quad (7)$$

$$\text{SINR}_i = \frac{|\mathbf{g}_i^H \mathbf{f}_i|^2}{\sum_{k \neq i} |\mathbf{g}_i^H \mathbf{f}_k|^2 + \sigma^2}, \quad (8)$$

where x_i is the unit-energy pilot symbol, $v_i \sim \mathcal{CN}(0, \sigma^2)$ denotes complex Gaussian noise, and $\mathbf{f}_k \in \mathbb{C}^{N \times 1}$ represents the beamforming vector of the k -th co-channel beam ($k \neq i$). The instantaneous per-beam link-quality metric SNR_i (or SINR_i under frequency reuse) computed from (2)–(8) is normalized to $[0, 1]$ and later used as part of the DRL observation vector.

C. Observation Model

In conventional beam-intersection methods, the UT location is inferred from the overlap of beam coverage regions. To build a unified and analytically tractable model, we define a set of differentiable measurements $\mathbf{z} \in \mathbb{R}^M$ that depend on the geometric distances between \mathbf{x} and the beam centers $\{\mathbf{c}_i\}$. For the i -th beam, a pseudorange-like measurement is modeled as

$$z_i = \|\mathbf{x} - \mathbf{c}_i\| + b + n_i, \quad (9)$$

where b represents the receiver clock bias and $n_i \sim \mathcal{N}(0, \sigma_i^2)$ is zero-mean Gaussian noise whose variance reflects the effective SNR of beam i .

Linearizing the pseudorange-like measurements in (9) at a reference \mathbf{x}_0 yields

$$\mathbf{z} \approx \mathbf{H} \mathbf{x} + b \mathbf{1} + \mathbf{n}, \quad (10)$$

where the i -th row of $\mathbf{H} \in \mathbb{R}^{M \times d}$ is \mathbf{h}_i^\top defined in (1), and $\mathbf{1} \in \mathbb{R}^{M \times 1}$.

D. Augmented Weighted Least Squares (WLS)

Let $\tilde{\mathbf{H}} = [\mathbf{H} \ \mathbf{1}] \in \mathbb{R}^{M \times (d+1)}$ and $\tilde{\mathbf{x}} = [\mathbf{x}^\top \ b]^\top$. Given $\mathbf{W} = \text{diag}(w_1, \dots, w_M)$, the augmented WLS estimate is

$$\hat{\tilde{\mathbf{x}}} = (\tilde{\mathbf{H}}^\top \mathbf{W} \tilde{\mathbf{H}} + \lambda \mathbf{I})^{-1} \tilde{\mathbf{H}}^\top \mathbf{W} \mathbf{z}, \quad (11)$$

with ridge parameter $\lambda > 0$ for numerical stability. We then parse $\hat{\mathbf{x}}$ and \hat{b} from $\hat{\tilde{\mathbf{x}}}$.

III. PROBLEM FORMULATION

From the system model above, the WLS estimator in (11) computes the UT position $\hat{\mathbf{x}}$ based on the beam-weight vector $\mathbf{w} = [w_1, \dots, w_M]^\top$. The instantaneous positioning error is defined as

$$e = \|\hat{\mathbf{x}} - \mathbf{x}_{\text{true}}\|_2. \quad (12)$$

The objective of the beam positioning problem is to find the optimal weight vector \mathbf{w}^* that minimizes the expected positioning error:

$$\mathbf{w}^* = \arg \min_{\mathbf{w} \in \mathcal{W}} \mathbb{E}[\|\hat{\mathbf{x}}(\mathbf{w}) - \mathbf{x}_{\text{true}}\|_2^2], \quad (13)$$

subject to $w_i \in [0, 1]$ and $\sum_i w_i = 1$, where \mathcal{W} denotes the feasible set of normalized weight vectors.

The above optimization is nonlinear and highly dependent on the beam geometry through the matrix \mathbf{H} in (10). Since \mathbf{H} varies rapidly with satellite motion and beam scheduling, solving (13) analytically or by exhaustive search is computationally prohibitive. Conventional heuristic methods assign fixed or power-based weights that cannot adapt to dynamic link conditions.

To overcome these limitations, we reformulate the beam-weight optimization as a sequential decision-making problem, where an agent learns to adjust \mathbf{w} based on observed beam features and positioning feedback. This motivates the proposed DRL approach detailed in Section IV. The continuous weight vector is discretized into a finite set of beam-selection and coarse-weight combinations to ensure tractable DQN training while maintaining sufficient action granularity.

IV. DQN-WLS BASED BEAM POSITIONING

In this section, we present a DRL framework that integrates a DQN with a WLS estimator for accurate and adaptive beam-based positioning in LEO satellite systems. Unlike conventional geometry- or CSI-based methods, the proposed DQN-WLS scheme dynamically learns beam-weighting strategies directly from uplink pilot responses, thus eliminating explicit CSI estimation and reducing computational complexity.

A. Markov Decision Process Formulation

The beam-weight optimization problem in (13) is reformulated as a Markov decision process (MDP) $\langle \mathcal{S}, \mathcal{A}, \mathcal{P}, \mathcal{R}, \gamma \rangle$. At each discrete time step t , the environment (*BeamEnv*) generates a state vector $\mathbf{s}_t \in \mathcal{S}$ that encapsulates both geometric and signal-level features of M visible beams. These include normalized beam distances, azimuth-elevation indicators, per-beam SINR metrics, previous residual errors, and prior weight distributions.

Action parameterization. To comply with DQN's discrete-action setting, we quantize the continuous beam weights into a finite action set constructed by top- K beam selections and coarse weight levels $\{0, 0.25, 0.5, 0.75, 1\}$, followed by ℓ_1 normalization. Near-duplicate actions are pruned by correlation screening to keep the action set tractable.

The agent selects a discrete action $a_t \in \mathcal{A}$, which is mapped to a normalized weight vector \mathbf{w}_t applied to the

WLS estimator. After performing the WLS estimation $\hat{\mathbf{x}}_t$, the environment computes the positioning error $e_t = \|\hat{\mathbf{x}}_t - \mathbf{x}_{\text{true}}\|_2$ and generates a scalar reward r_t that reflects both accuracy and stability:

$$r_t = -\left(\frac{e_t}{\tau}\right)^2 - \alpha \sum_{i=1}^M w_{t,i}(1 - \text{SINR}_i) - \beta(1 - \text{Entropy}(\mathbf{w}_t)), \quad (14)$$

where the entropy term is defined as

$$\text{Entropy}(\mathbf{w}_t) = -\sum_{i=1}^M w_{t,i} \log w_{t,i}, \quad (15)$$

which encourages exploration by promoting weight diversity. Here, τ controls the error-scaling factor, α penalizes low-quality beams, and β regulates the entropy contribution. The discount factor $\gamma = 0.99$ encourages long-term optimization over sequential interactions.

B. Network Architecture

The DQN approximates the action-value function $Q_\theta(\mathbf{s}, \mathbf{a})$ parameterized by θ . The input layer concatenates all beam-level features with a total feature dimension $F = 60$ for $M = 10$ beams. Two fully connected hidden layers of 128 neurons each, activated by ReLU, are used to extract latent geometric representations. After pruning redundant combinations, the discrete action set contains approximately 10^2 valid beam-weight configurations. The network outputs $|\mathcal{A}|$ Q-values over these quantized actions, and the selected action is mapped to a normalized weight vector \mathbf{w}_t .

To stabilize the subsequent WLS inversion, a ridge term $\lambda \mathbf{I}$ is added to (11). The network parameters are initialized using He initialization, optimized via Adam with learning rate $\eta = 10^{-3}$, and updated using the Huber loss. A target network $Q_{\bar{\theta}}$ is periodically synchronized with the main network Q_θ every $C = 200$ iterations to mitigate oscillations in temporal-difference targets.

C. Training Procedure

During training, the agent interacts with the environment over multiple episodes. At each step t , the agent observes the current state \mathbf{s}_t , selects an action $\mathbf{w}_t = f_\theta(\mathbf{s}_t)$ according to an ϵ -greedy policy, applies \mathbf{w}_t to the WLS estimator, and receives a reward r_t and next state \mathbf{s}_{t+1} . Each transition $(\mathbf{s}_t, \mathbf{w}_t, r_t, \mathbf{s}_{t+1})$ is stored in a replay buffer \mathcal{D} of size 10^4 . Mini-batches of 32 samples are randomly drawn from \mathcal{D} to update the network parameters.

The target value for each sample is defined as

$$y_t = r_t + \gamma Q_{\bar{\theta}}(\mathbf{s}_{t+1}, f_{\bar{\theta}}(\mathbf{s}_{t+1})), \quad (16)$$

and the temporal-difference (TD) loss follows the Huber formulation:

$$L_t(\theta) = \begin{cases} \frac{1}{2} \delta_t^2, & |\delta_t| < 1, \\ |\delta_t| - \frac{1}{2}, & \text{otherwise,} \end{cases} \quad (17)$$

where $\delta_t = y_t - Q_\theta(\mathbf{s}_t, \mathbf{w}_t)$. Gradients are clipped with $\|\nabla_\theta\| \leq 5$ to prevent divergence, and ϵ decays exponentially

Algorithm 1: DQN-WLS Based Beam Positioning

Input: Environment BeamEnv, learning rate η , discount factor γ , target update interval C , exploration schedule ϵ

Output: Trained DQN policy π_θ for adaptive beam-weighting

```
1 Initialize replay buffer  $\mathcal{D}$ , networks  $Q_\theta$  and target  $Q_{\bar{\theta}} \leftarrow Q_\theta$ ;  
2 for  $episode = 1$  to  $E_{\max}$  do  
3   Reset environment and obtain initial state  $s_0$ ;  
4   for each time step  $t$  do  
5     Select action  $w_t \leftarrow f_\theta(s_t)$  and apply  $\epsilon$ -greedy exploration;  
6     Normalize  $w_t$  s.t.  $\sum_i w_{t,i} = 1$ , form  $W_t = \text{diag}(w_t)$ ;  
7     Compute  $\hat{x}_t$  via WLS in (11);  
8     Compute positioning error  $e_t$  using (12);  
9     Evaluate reward  $r_t$  via (14) and observe next state  $s_{t+1}$ ;  
10    Store  $(s_t, w_t, r_t, s_{t+1})$  in buffer  $\mathcal{D}$ ;  
11    Sample mini-batch from  $\mathcal{D}$ ;  
12    Compute target  $y_t$  using (16);  
13    Update  $\theta \leftarrow \theta - \eta \nabla_\theta L_t(\theta)$  via Huber loss (17);  
14    if  $\text{mod}(t, C) = 0$  then  
15      | update target network  $Q_{\bar{\theta}} \leftarrow Q_\theta$ ;  
16    end  
17    if convergence or terminal state reached then  
18      | break;  
19    end  
20  end  
21 end  
22 return Optimal policy  $\pi_\theta^*$  generating  $w_t^*$  for each  $s_t$ 
```

from 1.0 to 0.01 during training. Convergence is typically achieved within 800 to 1000 episodes, after which the mean positioning error stabilizes below 0.05 m. Furthermore, the learned beam weights exhibit strong interpretability: high-SINR beams receive larger weights, while redundant or correlated beams are automatically suppressed, indicating that the agent implicitly learns the beam-geometry reliability without explicit CSI modeling.

V. SIMULATION RESULTS AND ANALYSIS

A. Experimental Setup

All simulations were conducted in Python using the PyTorch 2.5 framework on a workstation equipped with an Intel i9 CPU and an NVIDIA RTX A6000 GPU. A 2-D coverage area of 1000×1000 m² is considered with $M = 10$ visible beams. The discount factor is set to $\gamma = 0.99$, the learning rate $\eta = 10^{-3}$ (Adam optimizer), and the target network update interval $C = 200$. Each training episode consists of $T = 100$ steps, and the replay buffer stores 10^4 transitions. Six algorithms are compared for performance evaluation:

- **PPO [14]:** Proximal Policy Optimization baseline with a clipped surrogate objective.
- **DDQN [15]:** Double Deep Q-Network that employs separate target and online networks to mitigate overestimation.
- **DQN [11]:** Standard Deep Q-Network with experience replay and a single target estimator.
- **ALG-B [16]:** Geometry-based intersection and exclusion algorithm for massive-MIMO LEO constellations, utilizing beam footprints and satellite identifiers to determine user position.
- **LSTM-WLS [17]:** LSTM neural-network-based satellite weighting framework that predicts measurement reliability and applies adaptive WLS for single-epoch localization.
- **Proposed DQN-WLS:** The proposed method integrates adaptive beam weighting with the WLS estimator to enable without explicit CSI estimation, real-time positioning.

The implementation of all six algorithms, including network configurations and simulation parameters, is available for reproducibility.¹

B. Convergence Behavior

Fig. 1 illustrates the training convergence of cumulative reward and positioning error for the six algorithms across 1000 episodes. The PPO and DDQN models exhibit relatively unstable reward trajectories due to policy oscillation and overestimation bias, respectively. In particular, the DDQN agent shows limited improvement throughout training, which can be attributed to the quasi-continuous beam-weighting action space and the smooth reward landscape. Under such conditions, the value decoupling mechanism of DDQN provides limited benefit and may even slow convergence due to stale target updates, a phenomenon also observed in continuous control tasks. In contrast, the standard DQN achieves faster initial convergence but suffers from higher variance in later stages, indicating sensitivity to replay sampling. The proposed DQN-WLS demonstrates the most stable and rapid convergence, reaching a steady-state mean positioning error below 0.5 m within 800 episodes. This improvement stems from the adaptive beam-weighting mechanism that enables the agent to prioritize high-SINR beams while suppressing noisy or correlated ones. The geometry-guided regularization imposed by the WLS estimator further enhances training stability under dynamic multi-beam environments.

As a reference, the geometry-based ALG-B [16] and the LSTM-WLS [17] methods are not trained through episodic reinforcement learning. Hence, they do not appear in the convergence curves but are evaluated in subsequent subsections for accuracy and computational comparison. As illustrated in Fig. 1(d), the proposed agent achieves the highest reward stability and lowest error variance.

¹Source code and configuration files are available at: <https://github.com/BoneZhou/DRL-LEO-Beam-Positioning>

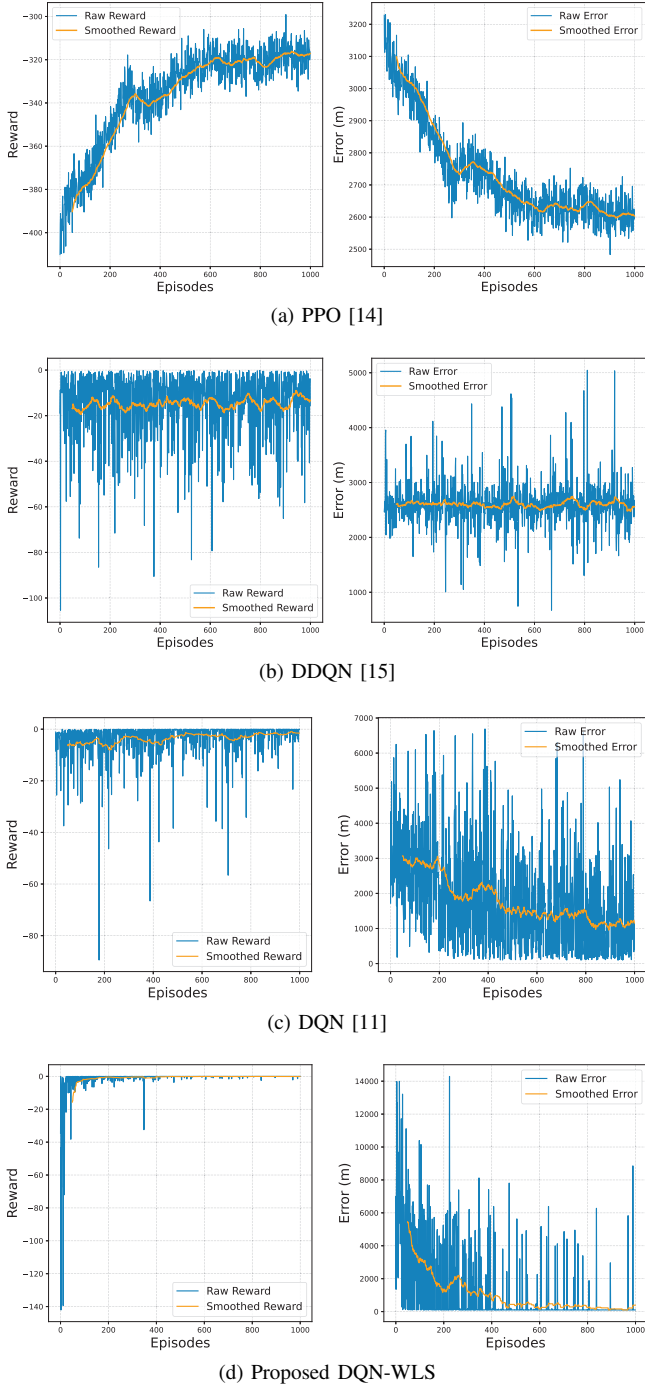


Fig. 1: Training convergence of cumulative reward and positioning error for PPO, DDQN, DQN, and the proposed DQN-WLS.

C. Positioning Visualization

Fig. 2 illustrates the final positioning results at Episode 1000 for three representative methods: the geometry-based ALG-B [16], the learning-based DQN [11], and the proposed DQN-WLS framework. As shown in Fig. 2(a), the ALG-B method produces a large localization deviation exceeding 10^4 m, since

TABLE I: Comparison of Positioning and Learning-Based Methods

Method	FLOPs (M)	Total FLOPs (G)	Time (s)	RMSE (m)
ALG-B [16]	—	—	2.61	3688.14
PPO [14]	0.07	92.87	3016.02	2558.33
DDQN [15]	0.04	77.59	350.08	2504.05
DQN [11]	0.02	18.94	13.52	10.38
LSTM-WLS [17]	31.24	78.09	262.96	0.01
Proposed DQN-WLS	0.02	18.95	9.43	0.395

it relies solely on fixed beam-intersection geometry without adaptive weighting or interference mitigation. The standard DQN in Fig. 2(b) reduces the error to the tens-of-meter level by learning partial beam reliability, but its positioning remains unstable due to the absence of explicit geometric constraints. In contrast, the proposed DQN-WLS shown in Fig. 2(c) achieves sub-meter accuracy (approximately 0.395 m) with near-perfect alignment between the estimated and true UT positions. The visual comparison highlights that integrating reinforcement learning with the WLS estimator enables robust and high-precision positioning without explicit CSI estimation.

D. Performance Comparison

Table I summarizes the overall computational and localization performance of six representative algorithms, including both geometric and learning-based approaches. The conventional beam-intersection method (ALG-B [16]) exhibits the largest localization deviation (> 3 km) due to its reliance on fixed beam footprints without adaptive weighting. Among DRL-based schemes, PPO [14] and DDQN [15] show unstable convergence and excessive computational overhead, while the standard DQN [11] significantly improves efficiency and reduces positioning error to 10.38 m. The LSTM-WLS [17] framework achieves extremely high accuracy (0.01 m) but incurs high training cost and longer inference latency, making it impractical for real-time onboard operation. By contrast, the proposed DQN-WLS achieves sub-meter accuracy (0.395 m) with the lowest runtime (9.43 s per episode) and nearly identical computational complexity to DQN (≈ 19 GFLOPs). These results confirm that integrating adaptive beam weighting with WLS estimation enables superior accuracy–efficiency trade-offs suitable for resource-constrained LEO satellite payloads. *Note:* FLOPs (M) denote per-inference forward FLOPs. Total (G) includes the complete training forward and backward passes under identical episode and batch settings. RMSE values are averaged over 10 seeds with fixed geometries and interference profiles.

E. Discussion

The superior performance of DQN-WLS arises from its hybrid nature, combining the adaptivity of deep reinforcement learning with the interpretability and stability of model-based estimation. Through interaction with the environment, the agent learns to emphasize high-SINR and geometrically diverse beams while suppressing redundant or noisy ones. This implicit weighting behavior, realized without explicit

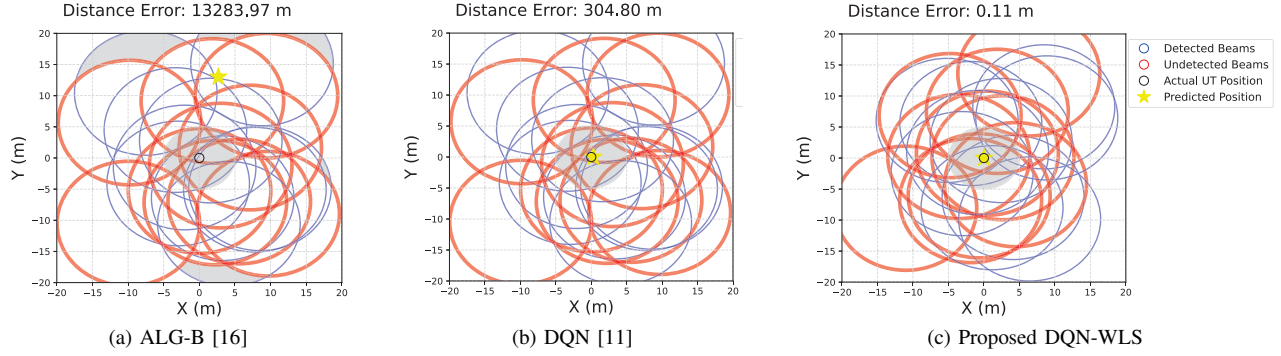


Fig. 2: Positioning visualization at Episode 1000 under identical beam geometry and noise conditions. The yellow star denotes the estimated UT position, and the black circle indicates the ground truth. Compared with the geometry-driven ALG-B and standard DQN, the proposed DQN-WLS aligns closely with the ground truth and yields the smallest residual error.

CSI, ensures geometric consistency and robust convergence across varying satellite-user topologies. Compared with fully supervised models such as LSTM-WLS, DQN-WLS attains comparable accuracy but with over 80% lower computational cost, demonstrating its practicality for real-time onboard deployment in LEO constellations. The lightweight inference pipeline and small network footprint make DQN-WLS feasible for future satellite onboard processors.

VI. CONCLUSION

This paper proposed a DQN-WLS beam positioning framework for LEO satellite constellations that jointly optimizes beam weighting and user localization without explicit CSI estimation. Unlike geometric intersection or purely data-driven approaches, the proposed hybrid method leverages reinforcement learning for adaptive beam selection and integrates WLS for physics-consistent position estimation. Comprehensive simulations show that DQN-WLS reduces the mean positioning error by 99.3% compared with existing DRL baselines and achieves a near-real-time inference latency of less than 10 s. Given its low complexity, scalability, and interpretability, the proposed framework offers a promising foundation for future onboard and autonomous beam management in next-generation non-terrestrial networks.

REFERENCES

- [1] S. Saleh, P. Zheng, X. Liu, H. Chen, M. F. Keskin, B. Priyanto, M. Beale, Y. Etefagh, G. Seco-Granados, T. Y. Al-Naffouri, and H. Wymeersch, "Integrated 6G TN and NTN localization: Challenges, opportunities, and advancements," *IEEE Commun. Standards Mag.*, vol. 9, no. 2, pp. 63–71, 2025.
- [2] J. Zhu, Y. Sun, and M. Peng, "Beam management in LEO satellite networks with random traffic arrival and time-varying topology," *IEEE Trans. Veh. Technol.*, vol. 73, no. 9, pp. 13352–13367, Sept. 2024.
- [3] Y. Cao, S.-Y. Lien, Y.-C. Liang, and D. Niyato, "Toward intelligent non-terrestrial networks through symbiotic radio: A collaborative deep reinforcement learning scheme," *IEEE Netw.*, vol. 39, no. 1, pp. 211–219, 2025.
- [4] Z. Lin, Z. Ni, L. Kuang, C. Jiang, and Z. Huang, "Multi-satellite beam hopping based on load balancing and interference avoidance for NGSO satellite communication systems," *IEEE Trans. Commun.*, vol. 71, no. 1, pp. 282–295, Jan. 2023.
- [5] J.-H. Lee, C. Park, S. Park, and A. F. Molisch, "Handover protocol learning for LEO satellite networks: Access delay and collision minimization," *IEEE Trans. Wireless Commun.*, vol. 23, no. 7, pp. 7624–7637, July 2024.
- [6] H. Xu, Y. Sun, Y. Zhao, M. Peng, and S. Zhang, "Joint beam scheduling and beamforming design for cooperative positioning in multi-beam LEO satellite networks," *IEEE Trans. Veh. Technol.*, vol. 73, no. 4, pp. 5276–5287, Apr. 2024.
- [7] A. Schröder, S. Gracla, M. Röper, D. Wübben, C. Bockelmann, and A. Dekorsy, "Flexible robust beamforming for multibeam satellite downlink using reinforcement learning," in *Proc. IEEE Int. Conf. Commun. (ICC)*, June 2024, pp. 3809–3814.
- [8] Y. Wang, Y. Chen, Y. Qiao, H. Luo, X. Wang, R. Li, and J. Wang, "Cooperative beam hopping for accurate positioning in ultra-dense LEO satellite networks," in *Proc. IEEE Int. Conf. Commun. Workshops (ICC Wkshps)*, June 2021, pp. 1–6.
- [9] A. Farajzadeh, A. Yadav, and H. Yanikomeroglu, "Federated learning in NTN: Design, architecture, and challenges," *IEEE Commun. Mag.*, vol. 63, no. 6, pp. 26–33, 2025.
- [10] S. M. Kay, *Fundamentals of Statistical Signal Processing, Volume I: Estimation Theory*. Prentice Hall, 1993.
- [11] V. Mnih *et al.*, "Human-level control through deep reinforcement learning," *Nature*, vol. 518, no. 7540, pp. 529–533, 2015.
- [12] E. D. Kaplan and C. J. Hegarty, *Understanding GPS/GNSS: Principles and Applications*, 3rd ed. Norwood, MA, USA: Artech House, 2017.
- [13] R. Shafin, L. Liu, Y. Li, Y. Li, A. Wang, and J. Zhang, "Angle and delay estimation for 3-D massive MIMO/FD-MIMO systems based on parametric channel modeling," *IEEE Trans. Wireless Commun.*, vol. 16, no. 8, pp. 5370–5383, Aug. 2017.
- [14] J. Schulman, F. Wolski, P. Dhariwal, A. Radford, and O. Klimov, "Proximal policy optimization algorithms," *arXiv preprint arXiv:1707.06347*, 2017.
- [15] H. van Hasselt, A. Guez, and D. Silver, "Deep reinforcement learning with double Q-learning," in *Proc. AAAI Conf. Artif. Intell.*, Feb. 2016, pp. 2094–2100.
- [16] M. Elsanhoury, J. Koljonen, M. Elmusrati, and H. Kuusniemi, "A novel beam-based positioning paradigm via opportunistic signal of future massive MIMO LEO satellite constellations," in *Proc. IEEE Int. Conf. Localization and GNSS (ICL-GNSS)*, Antwerp, Belgium, 2024, pp. 1–5.
- [17] I. Sbeity, C. Villien, C. Combettes, B. Denis, E. V. Belmega, and M. Chafii, "A novel satellite selection algorithm using LSTM neural networks for single-epoch localization," in *Proc. IEEE/ION Position, Location and Navigation Symp. (PLANS)*, Monterey, CA, USA, 2023, pp. 105–112.